Substituent effects on the reactivity of the silicon–carbon double bond. Arrhenius parameters for the reaction of 1,1-diarylsilenes with alcohols and acetic acid

Christine J. Bradaric and William J. Leigh

Abstract: Absolute rate constants for the reaction of a series of ring-substituted 1,1-diphenylsilene derivatives with methanol, *tert*-butanol, and acetic acid in acetonitrile solution have been determined using nanosecond laser flash photolysis techniques. The three reactions exhibit small positive Hammett ρ-values at 23°C, consistent with a mechanism involving initial, reversible nucleophilic attack at silicon to form a σ-bonded complex that collapses to product via rate-limiting proton transfer. Deuterium kinetic isotope effects and Arrhenius parameters have been determined for the reactions of 1,1-di-(4-methylphenyl)silene and 1,1-di-(4-trifluoromethylphenyl)silene with methanol, and are compared to those for the parent compound. Proton transfer within the complex is dominated by entropic factors, resulting in negative activation energies for reaction. The trends in the data can be rationalized in terms of variations in the relative rate constants for reversion to reactants and proton transfer as a function of temperature and substituent. A comparison of the Arrhenius activation energies for reaction of acetic acid with 1,1-diphenylsilene (E_a = +1.9 ± 0.3 kcal/mol) and the more reactive di-trifluoromethyl analogue (E_a = +3.6 ± 0.5 kcal/mol) suggests that carboxylic acids also add by a stepwise mechanism, but with formation of the complex being rate determining.

Key words: silene, substituent effects, kinetics, Arrhenius, flash photolysis.

Résumé : Faisant appel aux techniques de photolyse éclair avec laser à la nanoseconde, on a déterminé les constantes de vitesse absolues pour les réactions d'une série de 1,1-diphénylsilènes substitués sur le cycle avec le méthanol, le *tert*-butanol et l'acide acétique en solutions dans l'acétonitrile. À 23°C, les trois réactions présentent des valeurs ρ de Hammett faiblement positives qui sont en accord avec un mécanisme impliquant une attaque initiale nucléophile réversible au niveau du silicium qui conduit à la formation d'un complexe à liaison σ qui se décompose en produit par le biais d'un transfert de proton qui est cinétiquement limitant. On a déterminé les effets isotopiques cinétiques du deutérium ainsi que les paramètres d'Arrhenius pour les réactions du 1,1-di-(4-méthylphényl)silène et du 1,1-(di-4-trifluorométhylphényl)silène avec le méthanol et on les a comparés avec les valeurs correspondantes du composé parent. Le transfert de proton dans le complexe est dominé par des facteurs entropiques; ceci conduit à des valeurs négatives pour les énergies d'activation de ces réactions. On peut rationaliser les tendances dans ces résultats en termes de variations dans les constantes de vitesse relatives pour la retransformation en réactifs et celle du transfert de proton en fonction de la température et du substituant. Une comparaison des énergies d'activation d'Arrhenius pour la réaction de l'acide acétique avec le 1,1-diphénylsilène (E_a = +1,9 ± 0,3 kcal/mol) et celle avec l'analogue plus réactif ditrifluorométhyle (E_a = +3,6 ± 0,5 kcal/mol) suggère que les acides carboxyliques s'additionnent aussi par un mécanisme par étapes; toutefois la formation du complexe serait toutefois l'étape cinétiquement limitante.

Mots clés : silène, effets de substituants, cinétique, Arrhenius, photolyse éclair.

[Traduit par la rédaction]

Introduction

The best-known reactions of silenes are [2+2]-dimerization and nucleophilic addition of alcohols (1–3). Since the very first experimental demonstrations that silenes are formed as reactive intermediates in the thermolysis (4) and (or) photolysis (5, 6) of silacyclobutanes and disilanes, the formation of 1,3- or 1,2-disilacyclobutanes from dimerization or alkoxysilanes from trapping with alcohols have come to be identified as classic indicators of silene involvement in the reactions of organosilicon compounds.

From a mechanistic standpoint, the reaction with alcohols has been more extensively studied (7–17). Wiberg published the first experimental evidence that alcohol nucleophilicity — and not acidity — is the main factor affecting the kinetics of the reaction, and suggested a mechanism involving complex-

Received May 25, 1997.

C.J. Bradaric and W.J. Leigh.[1] Department of Chemistry, McMaster University, 1280 Main Street West, Hamilton, ON L8S 4M1, Canada.

[1] Author to whom correspondence may be addressed. Telephone: (905) 525-9140, ext. 23485/23715. Fax: (905) 522-2509. E-mail: leigh@mcmaster.ca

Scheme 1.

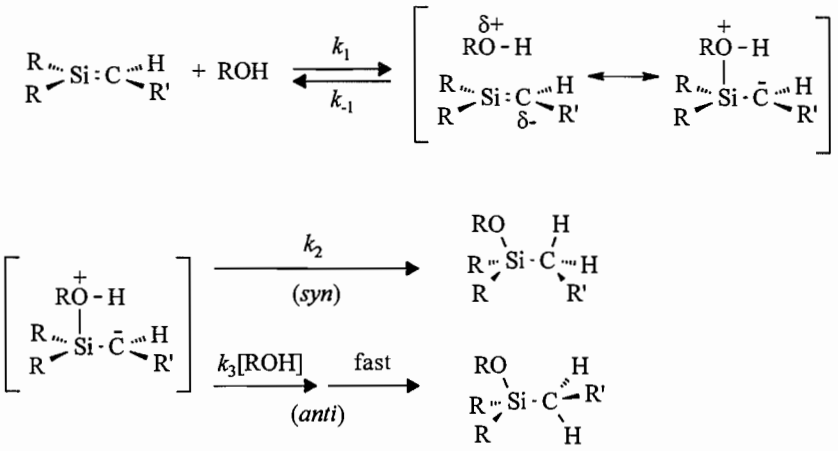

ation of the alcohol at silicon followed by proton transfer from oxygen to carbon (8). This was soon followed by reports of examples of both nonstereoselective (9) and stereoselective (11) alcohol additions, as well as an indication that in cases where more than one regio- or stereoisomeric product can be formed, the product distribution can vary with alcohol concentration (12). Sakurai and co-workers published the first comprehensive mechanism to explain these results (13), in a study of the effects of alcohol concentration on the ratio of *syn* and *anti* adducts obtained from reaction of various aliphatic alcohols with a cyclic, disilane-derived silene reactive intermediate. They proposed a refined version of Wiberg's mechanism, in which reaction is initiated with formation of a silene–alcohol complex, which proceeds to product by competing intracomplex (*syn*) and extracomplex (*anti*) proton-transfer pathways. The latter involves a second molecule of alcohol and hence increases in importance with increasing alcohol concentration. We have published kinetic and product studies for other transient silenes that support this mechanism (see Scheme 1), with the additional requirement that formation of the silene–alcohol complex be fully reversible (14–20). For each of the reactive silenes that we have studied, variations in solvent polarity and alcohol nucleophilicity, acidity, and isotopic substitution affect the kinetics and product distribution in ways that are fully compatible with this mechanism.

While theory suggests that substituents that reduce the natural polarity of the Si=C bond should lead to lower reactivity toward nucleophilic addition (10, 21), there has been little experimental effort directed toward developing a quantitative understanding of the effects of polar factors on silene reactivity. One relatively straightforward way of undertaking such a study would be through investigation of a series of ring-substituted 1,1-diphenylsilene derivatives (**2**), which might be generated by photolysis of the corresponding 1,1-diarylsilacyclobutanes (**1**) (6, 16, 17, 22–24). We have previously shown that the parent compound, 1,1-diphenylsilacyclobutane (**1a**), is a convenient source of 1,1-diphenylsilene (**2a**) for time-resolved spectroscopic studies, and have reported kinetic studies of the reactions of this silene with alcohols and acetic acid (16, 17).

In this paper, we report a study of the effects of ring substituents on the rate constants for addition of methanol, *tert*-butanol, and acetic acid to 1,1-diphenylsilene. We have employed the photocycloreversion of the series of 1,1-diarylsilacyclobutanes **1** to generate the corresponding silenes (**2**) in acetonitrile solution (eq. [1]), and have measured absolute rate constants, deuterium kinetic isotope effects, and Arrhenius parameters for reaction with these three reagents.

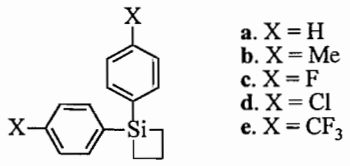

a. X = H
b. X = Me
c. X = F
d. X = Cl
e. X = CF_3

1

[1] 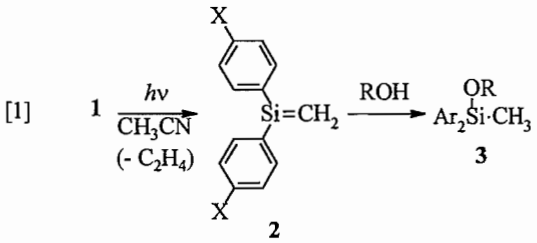

2 **3**

Results

Compounds **1b–e** were synthesized from 1,1-dichlorosilacyclobutane and the appropriate aryl magnesium bromide, using a method similar to that reported for the parent compound **1a** (17, 25). They were purified by column chromatography to >99% purity, and exhibited spectral and analytical data that are consistent with their assigned structures.

Direct irradiation of **1b–e** (0.007–0.013 M) in the presence of 0.05 M methanol results in the formation of the corresponding alkoxysilanes **3b–e** in high chemical yields.[2] No other products were observed in significant yield from the photoly-

[2] The 4,4′-dimethoxy analogue of **1** was also synthesized, but steady state photolysis of the compound under the same conditions yielded a number of products in minor yields. Furthermore, no evidence for the formation of the corresponding silene could be obtained by flash photolysis of the compound.

Table 1. Bimolecular rate constants, deuterium kinetic isotope effects, and Hammett ρ-values for reaction of 1,1-diarylsilenes (**2**) with MeOH, *t*-BuOH, and AcOH in deoxygenated acetonitrile solution at 23°C.[a]

2 (X)	k_{MeOH} (10^9 M^{-1} s^{-1})	$k_{t\text{-}BuOH}$ (10^9 M^{-1} s^{-1})	k_{AcOH} (10^9 M^{-1} s^{-1})
2b (X = Me)	1.12 ± 0.06	0.130 ± 0.006	1.41 ± 0.05
	(k_H/k_D = 1.9 ± 0.1)	(k_H/k_D = 1.9 ± 0.2)	(k_H/k_D = 1.2 ± 0.2)
2a (X = H)[b]	1.5 ± 0.1	0.22 ± 0.02	1.5 ± 0.2
	(k_H/k_D = 1.5 ± 0.1)	(k_H/k_D = 1.6 ± 0.1)	(k_H/k_D = 1.1 ± 0.1)
2c (X = F)	1.89 ± 0.08	0.33 ± 0.02	1.8 ± 0.2
2d (X = Cl)	2.13 ± 0.10	0.39 ± 0.02	2.0 ± 0.2
2e (X = CF_3)	2.99 ± 0.16	0.75 ± 0.04	2.3 ± 0.4
	(k_H/k_D = 1.0 ± 0.1)	(k_H/k_D = 1.7 ± 0.2)	(k_H/k_D = 1.1 ± 0.1)
ρ	+0.31 ± 0.05	+0.55 ± 0.08	+0.17 ± 0.02
	(r^2 = 0.980)	(r^2 = 0.985)	(r^2 = 0.987)

[a]Errors are listed as twice the standard deviation from least-squares analysis of k_{decay} – concentration data according to eq. [2].
[b]Data from ref. 17.

sis of any of the four compounds below ~40% conversion. The alkoxysilanes were isolated from the crude photolysis mixtures by semi-preparative GC, and identified on the basis of their NMR, IR, and mass spectra.

Nanosecond laser flash photolysis of continuously flowing, air-saturated solutions of **1b–e** (0.003–0.006 M) in acetonitrile affords weak, but readily detectable transient absorptions (λ_{max} ~ 325 nm) that decay with clean pseudo-first-order kinetics to within 10% of the pre-pulse level. The transients exhibit lifetimes in the 150–250 ns range in acetonitrile dried by distillation from calcium hydride, but these were extended to the 2–3 μs range using more scrupulously dried (i.e., $\leq 10^{-4}$ M water) samples of the solvent. The UV absorption spectra, lifetimes, and kinetic response of the transients to added silene quenchers (vide infra) are similar to those reported previously for 1,1-diphenylsilene, formed by photolysis of **1a** under similar conditions (17), and we thus assign them to the corresponding 1,1-diarylsilenes **2b–e**. For example, Fig. 1 shows the time-resolved UV absorption spectrum of **2e**, recorded 80–240 ns after the laser pulse for an air-saturated solution of **1e** in acetonitrile. As expected (17, 24), the lifetimes of the transients were not measurably shortened upon saturation of the solutions with oxygen.

Addition of methanol, *tert*-butanol, acetic acid, or water to the acetonitrile solutions of **1b–e** resulted in a reduction in the lifetimes of the 325-nm transient absorptions, consistent with their assignment to the silenes **2b–e**. Plots of the rate constant for decay (k_{decay}) versus concentration of added quencher (ROH) according to eq. [2] (where k_0 is the first-order rate constant for the decay of the transient in the absence of added quencher and k_{ROH} is the second-order quenching rate constant) were linear in all cases. Typical plots are shown in Fig. 2 for quenching of the four silenes by methanol. Similar experiments were carried out using MeOD, *t*-BuOD, and AcOD for **2b,e**. The absolute rate constants for reaction of silenes **2b–e** with MeOH, *t*-BuOH, and AcOH in acetonitrile are collected in Table 1, along with k_H/k_D values calculated from the data for the protiated and deuterated reagents. The corresponding data for **2a** (17) are included in the table for comparison.

Fig. 1. Time-resolved UV absorption spectrum recorded at 23 ± 1°C by nanosecond laser flash photolysis of an air-saturated acetonitrile solution of 1,1-di(4-trifluoromethylphenyl)silacyclobutane (**1e**, 0.0042 M). The spectrum was recorded over a time window of 80–240 ns after the laser pulse. The insert shows a typical decay trace, recorded at a monitoring wavelength of 325 nm.

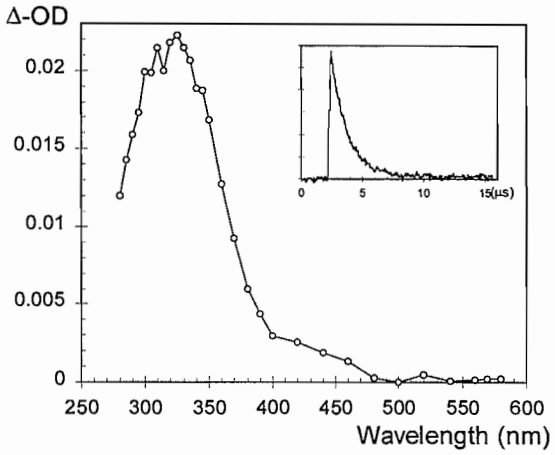

[2] $k_{decay} = k_0 + k_{ROH}[ROH]$

Absolute rate constants for reaction of silenes **2b** and **2e** with MeOH in acetonitrile were determined at several temperatures between −20°C and 55°C. Similar experiments were carried out for reaction of **2a** with MeOD and **2e** with HOAc in acetonitrile. The Arrhenius plots for quenching by MeOH(D) are shown in Fig. 3, along with that reported previously for quenching of **2a** by MeOH (16). Figure 4 shows the Arrhenius plots for quenching of **2a** (16) and **2e** with HOAc. Linear least-squares analysis of these data afforded the Arrhenius parameters collected in Table 2. In the case of **2e**–MeOH, only the data for temperatures above 13°C were employed for calculation of the Arrhenius parameters listed in the table. The Arrhenius plot for diffusion in acetonitrile, calculated using the modified Debye equation ($k_{diff} = 8RT/3000\eta$) and values

Table 2. Arrhenius activation parameters for addition of methanol, methanol-O-*d*, and acetic acid (ROL, where L = H or D) to selected 1,1-diarylsilenes (**2a**, **2b**, and **2e**) in acetonitrile solution.[a]

2 (X)	ROL	k_{ROL}^{25C} (10^9 M^{-1} s^{-1})[b]	$(k_H/k_D)^{23C}$	E_a (kcal mol^{-1})	log *A*	r^2
2b (X = Me)	MeOH	0.9 ± 0.1	1.9 ± 0.2	−2.7 ± 0.2	6.9 ± 0.3	0.973
2a (X = H)[c]	MeOH	1.3 ± 0.1	1.9 ± 0.2	−2.5 ± 0.3	7.3 ± 0.2	0.983
	MeOD	0.7	—	−3.2 ± 0.3	6.5 ± 0.2	0.979
	HOAc	1.3 ± 0.3	1.1 ± 0.1	1.9 ± 0.3	10.5 ± 0.4	0.982
2e (X = CF_3)	MeOH	2.2 ± 0.3	1.0 ± 0.1	−1.9 ± 0.2[d]	7.9 ± 0.1[d]	0.996
	HOAc	2.2 ± 0.2	[e]	3.6 ± 0.5	12.0 ± 0.4	0.980

[a]Errors are listed as twice the standard deviation from least-squares analysis of k_{decay} – concentration data according to eq. [2].
[b]Interpolated from Arrhenius data.
[c]Data from ref. 16.
[d]High temperature limiting values, from analysis of kinetic data obtained at $T > 13$°C.
[e]Not determined.

Fig. 2. Plots of ($k_{decay} - k_0$) versus [MeOH] from laser flash photolysis of air-saturated acetonitrile solutions of **1b–e** in the presence of methanol (X = Me, ■; X = F, ◆; X = Cl, Δ; X = CF_3, ●).

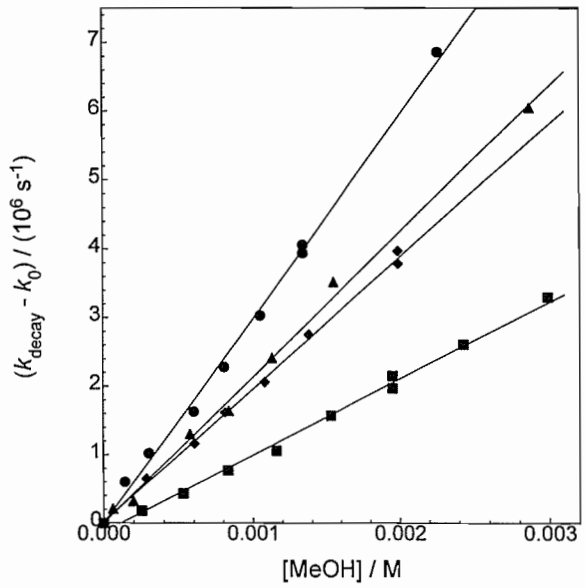

Fig. 3. Arrhenius plots for quenching of 1,1-diarylsilenes **2a** (X = H; ■), **2b** (X = Me; ◆), and **2e** (X = CF_3; ●) by methanol and **2a** by methanol-*O*-*d* (□) in acetonitrile solution. The **2a**-MeOH data are from ref. 16.

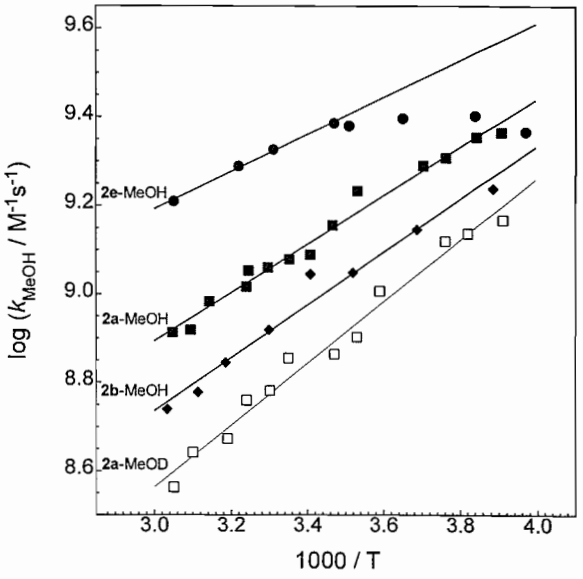

of η extrapolated from published temperature–viscosity data (26), is included in Fig. 4. Arrhenius parameters for addition of methanol to **2a** were also determined in hexane solution, from data recorded over a temperature range of −6–40°C. The values obtained are $E_a = -2.7 \pm 0.3$ kcal/mol and $\log A = 7.40 \pm 0.26$ ($r^2 = 0.996$). The rate constant for reaction at 23°C was found to be $(2.9 \pm 0.3) \times 10^9$ M^{-1} s^{-1}, in satisfactory agreement with our previously determined value (17).

Addition of 0.5 M methanol to nitrogen-saturated acetonitrile or hexane solutions of **1a,d,e** — enough to reduce the lifetimes of the corresponding silene to $\tau < 10$ ns — allowed the detection of weak residual signals that decayed with pseudo-first-order kinetics and lifetimes of 0.5–2 μs. The intensity of this signal was greatest in the case of the *para*-chloro compound **1d**, and for all three compounds was greater in hexane than in acetonitrile. The time-resolved absorption spectra of these transients showed $\lambda_{max} \sim 360$ nm in all cases, and the lifetimes proved to be sensitive to the presence of oxygen or 1,3-octadiene. Plots of the observed transient decay rate constants versus diene concentration were linear, and afforded quenching rate constants in the range (3–4) × 10^9 M^{-1} s^{-1} in hexane solution at 23°C. On the basis of these data, the transients observed under these conditions are assigned to the silacyclobutane triplet states. Addition of 0.01 M 1,3-octadiene to nitrogen-saturated solutions of **1a–e** in the absence of methanol resulted in no discernible change in either the lifetime or the initial absorbance of the transient signal assigned to the corresponding silene (at 325 nm), indicating that the formation of the silene does not involve the triplet state of the disilacyclobutane.

Fig. 4. Arrhenius plots for quenching of 1,1-diphenylsilene (**2a**; □) and 1,1-di-(4-trifluoromethylphenyl)silene (**2e**; ●) by acetic acid in acetonitrile solution. The data for **2a** are from ref. 16. The broken line corresponds to that for diffusion in acetonitrile, calculated using the modified Debye equation and published viscosity data (see text).

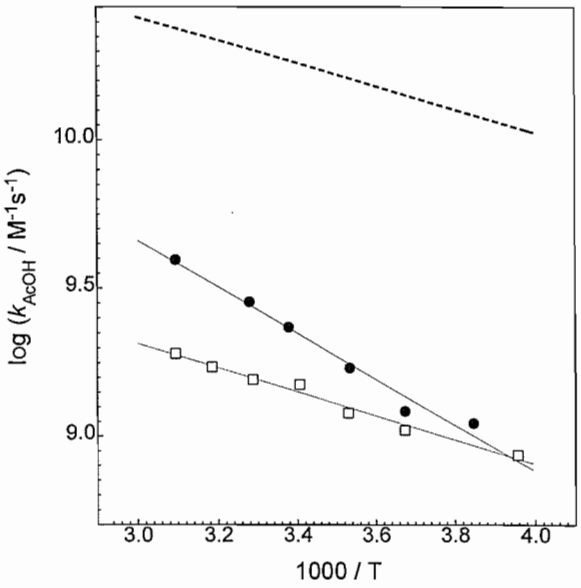

Discussion

The four substituted 1,1-diarylsilacyclobutanes studied in this work all exhibit analogous photochemical behaviour to that of the parent compound, 1,1-diphenylsilacyclobutane (**1a**). All five compounds yield the corresponding methoxydiarylmethylsilane (**3**) in high chemical yield upon direct irradiation in hexane or acetonitrile solution in the presence of methanol or other silene traps (27), consistent with the formation of the corresponding 1,1-diarylsilene (**2**). The rates of formation of the alkoxysilanes from photolysis of **1a–e** indicate that there is no appreciable variation throughout the series in the quantum yield for silene formation ($\Phi_2 = 0.24 \pm 0.03$ in the case of **1a** (17)). Intersystem crossing to yield the silacyclobutane triplet state also occurs, but this is relatively minor and is clearly unrelated to the formation of the silene by cycloreversion in the lowest excited singlet state.

The five silenes exhibit similar behaviour as well; they all exhibit long-wavelength absorption bands with $\lambda_{max} \sim 325$ nm, decay with pseudo-first-order kinetics in dried acetonitrile in the absence of (intentionally) added trapping reagents, and exhibit lifetimes in the 2–3 μs range. These lifetimes probably reflect limiting quenching by residual water in the solvent; since quenching of **2a** by water is as fast as by methanol (17), a concentration of only $\sim 10^{-4}$ M would result in a lifetime in the microsecond range. In agreement with this, the lifetimes vary slightly through the series, with that of **2b** being the longest and that of **2e** the shortest. The normal fate of **2a** in the absence of traps is dimerization (23, 25, 28), which should result in second-order decay kinetics. However, even in sodium-dried hexane, silene **2a** decays with mixed second- and pseudo-first-order kinetics. We conclude that dimerization of these silenes is relatively slow, probably due to steric factors.

The addition of alcohols to reactive silenes has received a great deal of attention over the past several years (7–17). As shown in Scheme 1, the mechanism is thought to involve initial nucleophilic attack at silicon followed by proton transfer from oxygen to carbon. A mechanism involving a silenium ion, formed by initial protonation at carbon, can be ruled out simply by the fact that the rate of reaction generally does *not* depend in a straightforward way on ROH acidity; the more important factor appears to be nucleophilicity (8, 14, 15, 17). The overall rate constant generally exhibits a small primary deuterium isotope effect, indicating that the initial intermediate (a zwitterionic silene–alcohol "complex") reverts to the free silene and alcohol at least as fast as it collapses to alkoxysilane by proton transfer (14, 15, 17). The involvement of this intermediate is further suggested by the fact that silenes characteristically form complexes with ethers (29). As well, several reactive silenes (including **2a**) have been found to exhibit negative activation energies in their reactions with methanol and (or) *tert*-butanol (16, 20, 30). While this is a common feature of fast reactions that proceed by mechanisms of this general type (31–40), it does not in itself rule out the possibility that the reaction proceeds by a concerted mechanism (32, 35, 37, 41–43).

The best evidence for the intermediacy of the σ-bonded complex in alcohol additions to silenes is the fact that the product distribution quite commonly varies with bulk alcohol concentration (12, 13, 15, 17). There is good evidence to suggest that this is due to proton transfer proceeding by two competing pathways: a unimolecular pathway involving [1,3]-proton migration within the complex, and a bimolecular pathway involving a second molecule of alcohol. This aspect of the mechanism was originally proposed on the basis of a study of the addition of various aliphatic alcohols to a cyclic transient silene, where it was found that for methanol, the stereochemistry of addition depends on bulk alcohol concentration (13). *syn*-Addition predominates at low alcohol concentrations where the intracomplex (unimolecular) proton transfer pathway should be operative, while *anti*-addition predominates at high alcohol concentrations due to increased importance from the extracomplex proton transfer pathway. *tert*-Butanol was found to add with 100% *syn*-stereochemistry at all alcohol concentrations, indicating that it reacts only by the unimolecular pathway in this particular case. Other workers, including us, have reported analogous concentration dependences in the *regio*chemistry of addition of aliphatic alcohols to conjugated silenes (12, 15). In the case of **2a**, the competing proton transfer pathways manifest themselves in competition experiments with methanol and *tert*-butanol, where the yield of the methanol adduct (relative to the *tert*-butanol adduct) increases with increasing bulk alcohol concentration (17). Sakurai and co-workers originally proposed that the bimolecular pathway involves protonation at carbon followed by rapid deprotonation from oxygen (13), but solvent and deuterium isotope effect studies seem more compatible with a deprotonation–protonation sequence (15, 17).

Kinetic studies have also provided evidence for a mechanism involving mixed first- and second-order dependences on alcohol concentration (14, 15), in the form of a quadratic variation in the pseudo-first-order rate constant for silene consumption (k_{decay}) with [ROH]. The expression shown in eq. [3], derived using the steady state assumption for the complex, collapses to a simple quadratic expression in [ROH] under

Fig. 5. Hammett plots for quenching of 1,1-diarylsilenes by MeOH (□), *t*-BuOH (◆), and AcOH (●) in acetonitrile solution.

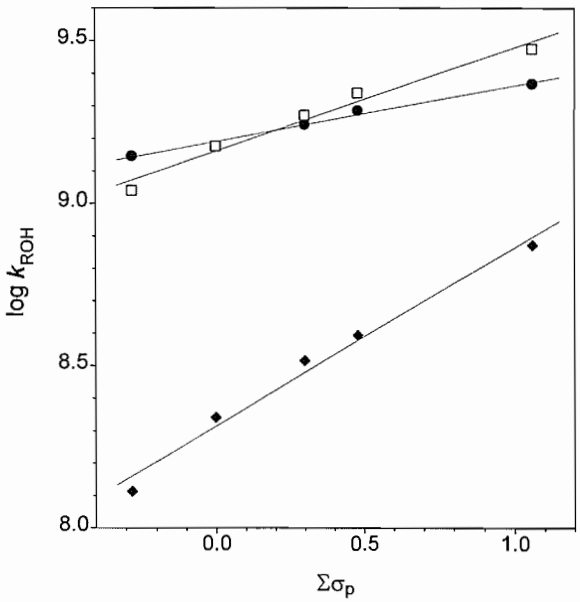

conditions where reversion of the complex to reactants is significantly faster than proton transfer (i.e., $k_{-1} > (k_2 + k_3[ROH])$) and uni- and bimolecular proton transfer proceed with comparable rate constants. Behaviour of this type has been reported for silenes in which conjugating substituents on the silenic carbon (14, 15) stabilize the complex toward intramolecular proton transfer. Simpler silenes such as **2a** (17) and others (16, 17, 20, 30)[3] exhibit higher overall reactivity toward alcohols, and show linear dependences of k_{decay} on [ROH] over the alcohol concentration ranges that can be studied using nanosecond time-resolved techniques.

$$[3] \quad k_{decay} = k_0 + \frac{k_1[ROH]}{(k_{-1} + k_2 + k_3[ROH])}(k_2 + k_3[ROH])$$

Not surprisingly, the latter behaviour is also observed for **2b–e** for quenching by both MeOH and *t*-BuOH (Fig. 2). It indicates that over the concentration ranges employed for our kinetic measurements (<0.01 M for MeOH; <0.05 M for *t*-BuOH), reaction occurs predominantly by the intracomplex proton transfer pathway for both alcohols. Under these conditions, the expression for k_{decay} simplifies to that in eq. [4].

$$[4] \quad k_{decay} = k_0 + \frac{k_1 k_2}{k_{-1} + k_2}[ROH]$$

The trends in the observed rate constants for reaction of **2a–e** with MeOH and *t*-BuOH indicate that electron-withdrawing substituents at silicon increase silenic reactivity toward alcohols, providing additional evidence for a mechanism in which nucleophilic attack at silicon precedes protonation at carbon. Hammett plots, shown in Fig. 5, afford ρ-values of +0.31 and +0.55 for reaction with MeOH and *t*-BuOH, respectively. The difference between the ρ-values for the two alcohols is small, presumably because the overall rate constants for both alcohols are so large. However, the effect is slightly greater for the less reactive alcohol, as would be expected.

To a first approximation, these reaction constants can be viewed as the sum of those of the individual complexation and proton transfer steps (see Scheme 1). The ρ-value for the complexation step would clearly be expected to be positive, while that for the proton transfer step should be small because the process involves charge neutralization within the zwitterionic complex. Thus, the positive overall reaction constants can be interpreted as reflecting mainly the effects of substituents on the initial reaction of the silene with the neutral nucleophile. This has obvious analogies to Michael addition reactions and, indeed, the addition of various nucleophiles such as amines (44), cyanide ion, and enolates (45) to substituted β-nitrostyrenes exhibit Hammett ρ-values in the range +0.2–1 depending on the nucleophile and the solvent.

The trend in the k_H/k_D values for reaction of methanol with **2a–e** (decreasing with increasing substituent electron-withdrawing power; see Table 1) can be explained in terms of variations in the relative magnitudes of the rate constants for reversion of the complex to reactants (k_{-1}) and collapse to product (k_2), since the isotope effect on k_1 should be a secondary one and indistinguishable from unity. The overall isotope effect is predicted to be a maximum in the limit of $k_{-1} >> k_2$ (i.e., fully reversible complex formation) and reduce in magnitude as k_{-1} decreases and (or) k_2 increases. Only a secondary isotope effect should be obtained in the limit of $k_2 >> k_{-1}$, where complex formation is fully rate determining. The data are consistent with an increase in the ratio k_2/k_{-1} with increasing substituent electron-withdrawing power, a trend which also manifests itself in the Arrhenius behaviour of the reactions of MeOH with **2a**, **2b**, and **2e**.

A reaction proceeding by a mechanism of the general type shown in Scheme 1 will exhibit a negative Arrhenius activation energy if the free energy of activation for the second step (in this case, proton transfer) is dominated by the entropic term, so that the enthalpy of the transition state is lower than that of the reactants. In addition, the first step must be reversible; i.e., reversion of the intermediate to reactants (k_{-1}) must be faster than its collapse to product (k_2) (31). If the opposite is true, then the first step is clearly the rate-determining step for reaction and the overall activation energy will be positive, of a value equal to or greater than that of diffusion (E_{diff}). The changeover from the situation where $k_{-1} >> k_2$ (E_a at the maximum negative value) to that where $k_{-1} << k$ (E_a at the maximum positive value) arises because the two reaction channels available to the intermediate have opposing entropic requirements (i.e., $\Delta S_{-1}^{\neq} > 0$ and $\Delta S_2^{\neq} < 0$) and the enthalpic barrier for product formation is small. Provided that a large enough temperature range can be spanned experimentally, the Arrhenius plot for a situation of this type should thus be bell shaped, with the region of the apex in the plot corresponding to the temperature range where k_{-1} is comparable to k_2 (34, 36). In the present case where the second step involves proton transfer, the primary isotope effect on k_{obs} would be predicted to decrease with decreasing temperature from its maximum value at the high-temperature limit (i.e., where $k_{-1} >> k_2$),

[3] Also, R. Boukherroub, C.J. Bradaric, C. Cserti, and W.J. Leigh. To be published.

reducing to a secondary effect as k_2 overtakes k_{-1} in magnitude.

The Arrhenius plot for reaction of **2e** with methanol (Fig. 3) shows precisely this behaviour, exhibiting an apparent negative activation energy at temperatures above ~13°C and distinct curvature over the −20–13°C temperature range as the rate of product formation (k_2) approaches and then surpasses that of reversion of the complex to reactants. The less negative value of the high-temperature E_a observed for this compound compared to those for **2a,b** probably results from the fact that complex formation is not fully reversible over the limited "high-temperature" range examined. In the case of **2a**, and more so with **2b**, k_{-1} is proportionately larger than k_2 over our high-temperature range, resulting in larger negative values of the apparent activation energy. Silene **2e** exhibits no significant deuterium isotope effect at 23°C, because this temperature is within the range where the rate constant is starting to be dominated by that of complex formation. We have not measured k_H/k_D at higher temperatures for this derivative, but as Fig. 3 illustrates, the deuterium kinetic isotope effect on the reaction of the parent compound (**2a**) with methanol increases as predicted with increasing temperature. The difference in the slopes of these two lines is significant at the 95% confidence level.

The relative placement of the Arrhenius plots shown in Fig. 3 for **2e**, **2a**, and **2b** can also be explained simply in terms of a successive decrease in the magnitude of k_2/k_{-1} throughout the series **2e** > **2a** > **2b**, as the trend in the isotope effects suggests. One might also expect the rate constant for complex formation (k_1) to decrease in the same order, provided that it is not diffusion controlled; this would contribute to the relative placement of the Arrhenius plots in the same way as the proposed variation in k_2/k_{-1}. Unfortunately, determination of k_1 for these compounds would require rate constant measurements at temperatures that are considerably below the present capability of our system. Given the placement of the −20°C point in relation to the apex of the plot, the measured value of k_{obs} for **2e** at −20°C (~ 2.2×10^9 M^{-1} s^{-1}) is expected to be a factor of 2–3 lower than the actual value of k_1 for this compound at this temperature. This suggests that $k_1 \sim 5 \times 10^9$ M^{-1} s^{-1}, a value very close to the diffusional rate constant (k_{diff} ~ 1×10^{10} M^{-1} s^{-1}), calculated using the modified Debye equation ($k_{diff} = 8RT/3000\eta$) and a value of η extrapolated from published temperature–viscosity data (26). Given the assumptions inherent in the Debye treatment, we conclude that formation of the methanol complex of **2e** is subject to at most a small barrier in excess of that of diffusion. The fact that the low-temperature data for the three compounds are clearly not converging to a single line suggests that k_1 is somewhat sensitive to substituent, and provides a better indication that, in general, the rate constant for complex formation is lower than that of diffusion.

The observed rate constant for reaction of **2a** with MeOH is about a factor of two higher in hexane than in acetonitrile, which is somewhat surprising since the more polar solvent might be expected to enhance reactivity through stabilization of the complex relative to reactants. However, the fact that the apparent E_a is less negative in acetonitrile than in hexane suggests that the opposite is true, probably as a result of weak Lewis acid–base complexation between the nitrile solvent and the silene.

Acetic acid invariably reacts with silenes with clean overall second-order kinetics, and rate constants that are generally larger than those for reaction with methanol (14, 15, 19). However, the reaction does not exhibit an isotope effect distinguishable from unity and, with **2a**, it exhibits a small positive Arrhenius activation energy (16). In this case, the carbonyl oxygen is the likely site of bonding to silicon, in which case proton transfer would occur via a six-membered transition state. The data are compatible with a stepwise mechanism analogous to that for alcohol additions, but with complex formation being fully rate determining. Complex formation should be slower with HOAc than MeOH because of its lower nucleophilicity (as estimated from the pK_b's in acetonitrile (46)), while proton transfer would clearly be expected to be much faster. However, it is difficult to rule out a concerted mechanism in this case since little isotope effect would be expected for such a strongly exothermic reaction.

The Hammett ρ-value of +0.17 observed for the reactions of **2a–e** with HOAc at 23°C indicates the reaction to be relatively insensitive to polar factors, a result which seems more consistent with a concerted addition mechanism. However, the fact that the Arrhenius activation energy for addition to the most reactive compound (**2e**) is *higher* than that of **2a** indicates otherwise. As mentioned above, the full Arrhenius plot is expected to be bell shaped, with an extended temperature region where the mechanistic changeover occurs from rate-determining proton transfer (at high temperatures) to rate-determining complex formation (at low temperatures). The smaller apparent activation energy observed for **2a** may result

[5] 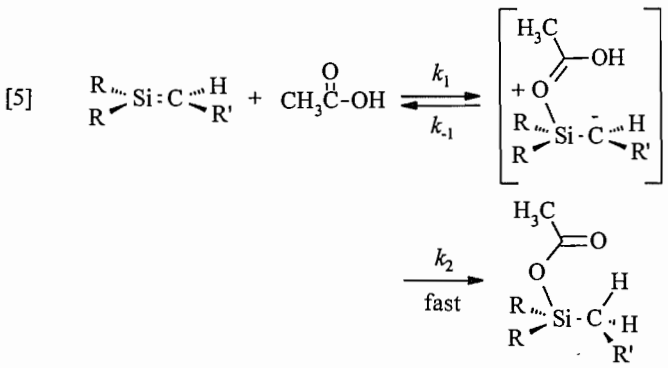

simply from the fact that the temperature range monitored is within that over which reversion of the complex to reactants is still marginally competitive with collapse to product. With **2e**, a larger k_1 and larger k_2/k_{-1} ratio would result in a shift in the "peak" of the Arrhenius plot to higher temperatures (as is observed for MeOH addition). Thus, over the temperature range monitored for the two compounds, we are simply observing the region of steeper temperature dependence of k_{obs} in the case of **2e**, compared to the situation with **2a**. If this explanation is correct, then the measured Arrhenius parameters for **2e** ($E_a = 3.6 \pm 0.5$; log A = 12.0 ± 0.4; $\Delta S^{\neq}_{23C} = -6 \pm 2$ cal deg^{-1} mol^{-1}) more closely reflect those for formation of its complex with HOAc than do those for **2a** ($E_a = 1.9 \pm 0.2$; log $A = 10.5 \pm 0.2$; $\Delta S^{\neq}_{23C} = -12.5 \pm 0.9$ cal deg^{-1} mol^{-1}). The activation energy for reaction of **2e** is significantly higher than that for diffusion ($E_a = 1.8 \pm 0.4$; log $A = 11.6 \pm 0.5$), indicating the presence of a small enthalpic barrier for complex formation. The data of Fig. 4 indicate that the sensitivity

of the overall rate constant for HOAc addition to ring substituents increases at higher temperatures, where reversibility of complex formation is a more important contributor to the magnitude of k_{obs}.

Summary and conclusions

The effects of ring substituents on the rate constants, deuterium kinetic isotope effects, and Arrhenius parameters for addition of aliphatic alcohols to 1,1-diphenylsilene are most easily explained in terms of a mechanism involving fast, reversible formation of a zwitterionic silene–alcohol complex, followed by rate-limiting proton transfer from oxygen to carbon (Scheme 1). Because the Arrhenius activation energies for the reaction with methanol are consistently negative, little quantitative information on the enthalpies and entropies of activation for the individual steps in the sequence can be obtained. Nevertheless, the variation in Arrhenius behaviour and isotope effect as a function of substituent indicates that electron-withdrawing substituents at silicon increase both the rate at which the complex is formed and the relative rates of its collapse to alkoxysilane product and reversion to starting materials. In extreme cases, this results in a change in the identity of the slower step from proton transfer to complex formation over the temperature range studied (−20–50°C), allowing observation of the bell-shaped Arrhenius plot that is predicted for a mechanism of this type.

Addition of acetic acid, which yields the corresponding acetoxyaryldimethylsilane (17), proceeds with overall rate constants that are similar in magnitude to those for methanol addition but vary less with substituent ($\rho = +0.17 \pm 0.02$). These reactions exhibit isotope effects indistinguishable from unity and positive Arrhenius activation energies, consistent with complex formation being rate determining. The activation energy for reaction *increases* with increased silene reactivity, which is most easily explained in terms of the stepwise mechanism. Our results indicate there to be a small but significantly higher enthalpic barrier to complex formation than is the case for methanol addition.

Further studies of the effects of substituents on the reactivity of the Si=C bond are in progress in our laboratory.

Experimental

NMR spectra were recorded in deuteriochloroform and are referenced to tetramethylsilane. ^{1}H and ^{13}C NMR spectra were recorded on a Bruker AC200 spectrometer, while ^{29}Si NMR spectra were recorded on Bruker DRX500 or AC300 spectrometers in deuterated chloroform solution; all are referenced to tetramethylsilane. Ultraviolet absorption spectra were recorded on Hewlett–Packard HP8451 or Perkin Elmer Lambda 9 spectrometers. Low-resolution mass spectra were determined by GC–MS, using a Hewlett–Packard 5890II gas chromatograph equipped with a HP-5971A mass selective detector and DB-5 fused silica capillary column (30 m × 0.25 mm; Chromatographic Specialties, Inc). High-resolution desorption electron impact (DEI) mass spectra and Exact Masses were recorded on a VGH ZABE mass spectrometer. Exact Masses employed a mass of 12.000000 for carbon. Infrared spectra were recorded as thin films on a BioRad FTS-40 FTIR spectrometer and are reported in wave numbers (cm^{-1}).

Analytical gas chromatographic analyses were carried out using a Hewlett–Packard 5890 gas chromatograph equipped with conventional heated splitless injector, a flame ionization detector, a Hewlett–Packard 3396A integrator, and a DB1701 megabore capillary column (15 m × 0.53 mm; Chromatographic Specialties, Inc.). Semi-preparative gas chromatographic separations were carried out using a Varian 3300 gas chromatograph equipped with a thermal conductivity detector and a metal column (3% OV 101 on Chromosorb W, HP 80/100; 6 ft × 0.25 in; Chromatographic Specialties, Inc.).

Acetonitrile (BDH or Caledon Reagent) was refluxed over calcium hydride (Fisher) for several days, distilled under dry nitrogen, and then cycled three times through a 1 in. × 6 in. column of neutral alumina (Aldrich) that had been activated by heating under vacuum (ca. 0.05 Torr; 1 Torr = 133.3 Pa) at 320°C for 10 h with periodic shaking. Methanol (Sigma Aldrich HPLC; <0.05% H_2O) and *tert*-butyl alcohol (Sigma Aldrich HPLC; <0.05% H_2O) were stored over activated 4 Å molecular sieves. Hexane (EM Science Omnisolv), glacial acetic acid (Caledon Reagent), and deuterated reagents (Isotec, Inc.) were used as received from the suppliers.

The 1,1-diarylsilacyclobutanes **1b–1e** were prepared from 1,1-dichlorosilacyclobutane and the appropriate aryl magnesium bromide, according to the published method for **1a** (17, 25). The only significant variation in procedure was the reaction time, which decreased from 8 h for **1b** to 5 h for **1e**. The diarylsilacyclobutanes were obtained as colourless oils, in yields of 50–90% after purification by column chromatography on silica gel. Each contained <0.01% of the corresponding 1,1-biaryl derivative as determined by capillary gas chromatography. Spectral and analytical data for the diarylsilacyclobutanes are listed below.

*1,1-Di-(4-methylphenyl)silacyclobutane (**1b**)*: IR: 3067 (s), 3035 (s), 3013 (s), 2990 (s), 1603 (s), 1501 (s), 1394 (s), 1121 (s), 1081 (s), 854 (s), 716 (s), 634 (s); ^{1}H NMR, δ (ppm): 1.45 (t, 8.2 Hz, 4 H), 2.23 (p, 8.4 Hz, 2H), 2.36 (s, 6H), 7.20 (d, 7.8 Hz, 4H), 7.50 (d, 7.7 Hz, 8H); ^{13}C NMR, δ (ppm): 14.0, 18.3, 21.7, 128.8, 133.0, 134.6, 139.6; ^{29}Si NMR, δ (ppm): 6.51; MS, *m/e* (*I*): 252 (15), 226 (22), 224 (100), 211 (12), 209 (48), 160 (10) 119 (8). Exact Mass, calcd. for $C_{17}H_{20}Si$: 252.1334; found: 252.1346.

*1,1-Di-(4-fluorophenyl)silacyclobutane (**1c**)*: IR: 2971 (m), 2928 (s), 2875 (m), 1588 (s), 1500 (s), 1390 (m), 1236 (s), 1162 (s), 1123 (s), 1109 (s), 855 (s), 826 (s), 670 (s); ^{1}H NMR, δ (ppm): 1.46 (t, 8.3 Hz, 4H), 2.23 (p, 8.3 Hz, 2H), 7.08 (d, 8.7 Hz, 4H), 7.55 (d, 8.7 Hz, 4H); ^{13}C NMR, δ (ppm): 14.1, 18.1, 115.3, 131.7, 136.5, 164.2; ^{19}F NMR, δ (ppm): −110.1 (s); ^{29}Si NMR, δ (ppm): 6.60; MS, *m/e* (*I*): 260 (5), 233 (20), 232 (100), 231 (43), 219 (20), 217 (62), 183 (8), 165 (20), 164 (6), 152 (9), 151 (18), 150 (14), 123 (40), 75 (6). Exact Mass, calcd. for $C_{15}H_{14}SiF_2$: 260.0833; found: 260.0852.

*1,1-Di-(4-chlorophenyl)silacyclobutane (**1d**)*: IR: 2971 (m), 2927 (m), 1579 (s), 1483 (m), 1381 (m), 1121 (m), 1084 (s), 1015 (m), 853 (s), 713 (m), 677 (m); ^{1}H NMR, δ (ppm): 1.47 (t, 8.2 Hz, 4 H), 2.25 (p, 8.3 Hz, 2H), 7.37 (d, 8.2 Hz, 4H), 7.50 (d, 8.2 Hz, 8H); ^{13}C NMR, δ (ppm): 13.9, 18.2, 128.4, 134.2, 135.8, 136.3; ^{29}Si NMR, δ (ppm): 6.95; MS, *m/e* (*I*): 294 (8), 292 (10), 268 (15), 266 (70), 264 (100), 253 (18), 251 (45),

250 (40), 231 (10), 229 (25), 165 (20), 152 (10), 141 (15), 139 (45), 103 (8), 89 (8), 77 (8),65 (28), 63 (78). Exact Mass, calcd. for $C_{15}H_{14}SiCl_2$: 292.0242; found: 292.0239.

*1,1-Di-(4-trifluoromethylphenyl)silacyclobutane (**1e**)*: IR: 2974 (s), 2931 (s), 1392 (s), 1324 (s), 1166 (s), 1104 (s), 1060 (s), 1019 (s), 827 (s), 704 (s); ^{1}H NMR, δ (ppm): 1.56 (t, 8.3 Hz, 4 H), 2.31 (p, 8.3 Hz, 2H), 7.66 (d, 8.0 Hz, 4H), 7.72 (d, 8.0 Hz, 4H); ^{13}C NMR, δ (ppm): 13.6, 18.4, 124.1, 124.7, 132.0, 134.7, 140.4; ^{19}F NMR, δ (ppm): −62.7 (s); ^{29}Si NMR: δ (ppm): 7.73; MS, *m/e* (*I*): 360 (10), 341 (12), 333 (22), 332 (100), 319 (20), 317 (6), 263 (15), 251 (10), 173 (15), 140 (30). Exact Mass, calcd. for $C_{17}H_{14}SiF_6$: 360.0769; found: 360.0766.

Steady-state photolysis experiments were carried out using a Rayonet reactor containing five RPR2537 lamps. Quartz tubes (25 cm × 1.2 cm) containing hexane solutions (ca. 20 mL) of **1b–e** (0.007–0.013 M) and 0.05 M methanol were sealed with rubber septa and irradiated for 70–110 min, resulting in 40–75% conversion of **1** to a single detectable product in each case. The volatiles were stripped from the photolysates on the rotary evaporator, and the products were isolated by semipreparative GC. They were identified as **3b–e** on the basis of the following data.

*Di-(4-methylphenyl)methoxymethylsilane (**3b**)*: IR: 2959 (s), 2927 (s), 2860 (m), 1601 (m), 1550 (m), 1254 (m), 1112 (m), 1088 (m), 1006 (m), 979 (m); ^{1}H NMR, δ (ppm): 0.59 (s, 3H), 2.35 (s, 6H), 3.51 (s, 3H), 7.20 (d, 7.7 Hz, 4H), 7.49 (d, 7.8 Hz, 4H); ^{13}C NMR, δ (ppm): −3.4, 21.5, 46.2, 128.7, 133.3, 134.8, 139.8; ^{29}Si NMR, δ (ppm): −0.96; MS, *m/e* (*I*): 256 (6), 242 (21), 241 (100), 212 (5), 211 (23), 165 (11), 131 (11), 119 (13), 105 (8), 93 (6), 91 (7), 65 (5). Exact Mass, calcd. for $C_{16}H_{20}OSi$: 256.1283; found: 256.1287.

*Di-(4-fluorophenyl)methoxymethylsilane (**3c**)*: IR: 2962 (s), 2938 (s), 2835 (m), 1588 (s), 1499 (s), 1388 (s), 1110 (s), 878 (s), 824 (s), 756 (s); ^{1}H NMR, δ (ppm): 0.59 (s, 3H), 3.50 (s, 3H), 7.04 (d, 8.7 Hz, 4H), 7.50 (d, 8.8 Hz, 4H); ^{13}C NMR, δ (ppm): −3.6, 46.1, 115.0, 131.1,136.3, 164.1; ^{29}Si NMR, δ (ppm): −2.49; MS, *m/e* (*I*): 264 (10), 249 (100), 220 (8), 219 (42), 169 (8), 139 (16), 123 (11), 109 (6), 59 (12). Exact Mass, calcd. for $C_{14}H_{14}F_2OSi$: 264.0782; found: 264.0782.

*Di-(4-chlorophenyl)methoxymethylsilane (**3d**)*: IR: 2959 (s), 2928 (s), 2850 (m), 1602 (m), 1550 (m), 1260 (m), 1110 (m), 1088 (m), 1006 (m), 969 (m); ^{1}H NMR, δ (ppm): 0.62 (s, 3H), 3.52 (s, 3H), 7.38 (d, 8.3 Hz, 4H), 7.50 (d, 8.4Hz, 4H); ^{13}C NMR, δ (ppm): −3.6, 51.2, 128.3, 134.2, 135.7, 136.3; ^{29}Si NMR, δ (ppm): −2.67; MS, *m/e* (*I*): 298 (11), 296 (16), 285 (14), 284 (13), 283 (70), 282 (20), 281 (100), 253 (20), 251 (30), 185 (13), 157 (7), 155 (20), 152 (13), 139 (11), 125 (7), 91 (7), 75 (9), 65 (9), 63 (21), 59 (22). Exact Mass, calcd. for $C_{14}H_{14}Cl_2OSi$: 296.0191; found: 296.0185.

*Di-(4-trifluoromethylphenyl)methoxymethylsilane (**3e**)*: IR: 2959 (s), 2929 (s), 2841 (m), 1392 (m), 1325 (s), 1269 (m), 1168 (s), 1132 (s), 1088 (s), 1061 (s), 1019 (s), 909 (m), 813 (s), 760 (s), 735 (s), 703 (m); ^{1}H NMR, δ (ppm): 0.68 (s, 3H), 3.55 (s, 3H), 7.62 (d, 7.8 Hz, 4H), 7.66 (d, 7.7 Hz, 4H); ^{13}C NMR, δ (ppm): −3.9, 51.3, 124.6, 131.8, 132.1, 134.5, 139.8; ^{29}Si NMR, δ (ppm): −2.83; MS, *m/e* (*I*): 364 (5), 350 (21), 349 (100), 320 (7), 319 (34), 271 (7), 252 (11), 219 (19), 189 (22), 173 (8), 159 (6), 127 (12), 126 (27), 59 (15). Exact Mass, calcd. for $C_{16}H_{14}OSiF_6$: 364.0718; found: 364.0709.

Nanosecond laser flash photolysis experiments employed the pulses (248 nm; ca. 16 ns; 70–120 mJ) from a Lumonics 510 excimer laser, filled with F_2/Kr/He mixtures, and a microcomputer-controlled detection system (47). The system incorporates a brass sample holder whose temperature is controlled to within 0.1°C by a VWR 1166 constant-temperature circulating bath. Solutions were prepared at concentrations such that the absorbance at the excitation wavelength (248 nm) was ca. 0.7 (0.004 M) and were flowed continuously through a 3 × 7 mm Suprasil flow cell connected to a calibrated 100 mL reservoir. Solution temperatures were measured with a Teflon-coated copper–constantan thermocouple that was inserted directly into the flow cell. Quenchers were added directly to the reservoir by microlitre syringe as aliquots of standard solutions. Rate constants were calculated by linear least-squares analysis of decay rate – concentration data (6–10 points), which spanned at least a factor of 5 (usually more than 1 order of magnitude) in the transient decay rate. Errors are quoted as twice the standard deviation obtained from the least-squares analysis in each case.

Acknowledgments

We wish to thank the Natural Sciences and Engineering Research Council of Canada for financial support, and the McMaster Regional Centre for Mass Spectrometry for exact mass determinations.

References

1. G. Raabe and J. Michl. Chem. Rev. **85**, 419 (1985).
2. M.G. Steinmetz. Chem. Rev. **95**, 1527 (1995).
3. A.G. Brook and M.A. Brook. Adv. Organomet. Chem. **39**, 71 (1996).
4. L.E. Gusel'nikov and M.C. Flowers. J. Chem. Soc. Chem. Commun. 864 (1967).
5. P. Boudjouk, J.R. Roberts, C.M. Golino, and L.H. Sommer. J. Am. Chem. Soc. **94**, 7926 (1972).
6. P. Boudjouk and L.H. Sommer. J. Chem. Soc. Chem. Commun. 54 (1973).
7. S. Nagase and T. Kudo. J. Chem. Soc. Chem. Commun. 363 (1983).
8. N. Wiberg. J. Organomet. Chem. **273**, 141 (1984).
9. A.G. Brook, K.D. Safa, P.D. Lickiss, and K.M. Baines. J. Am. Chem. Soc. **107**, 4338 (1985).
10. S. Nagase, T. Kudo, and K. Ito. *In* Applied quantum chemistry. *Edited by* V.H.J. Smith, H.F. Schaefer, and K. Morokuma. D. Reidel, Dordrecht. 1986. p. 249.
11. P.R. Jones and T.F. Bates. J. Am. Chem. Soc. **109**, 913 (1987).
12. M.G. Steinmetz, B.S. Udayakumar, and M.S. Gordon. Organometallics, **8**, 530 (1989).
13. M. Kira, T. Maruyama, and H. Sakurai. J. Am. Chem. Soc. **113**, 3986 (1991).
14. G.W. Sluggett and W.J. Leigh. J. Am. Chem. Soc. **114**, 1195 (1992).
15. W.J. Leigh and G.W. Sluggett. J. Am. Chem. Soc. **116**, 10468 (1994).
16. C.J. Bradaric and W.J. Leigh. J. Am. Chem. Soc. **118**, 8971 (1996).

17. W.J. Leigh, C.J. Bradaric, C. Kerst, and J.H. Banisch. Organometallics, **15**, 2246 (1996).
18. C. Kerst, C.W. Rogers, R. Ruffolo, and W.J. Leigh. J. Am. Chem. Soc. **119**, 466 (1997).
19. C. Kerst, R. Ruffolo, and W.J. Leigh. Organometallics, In press.
20. C. Kerst, R. Boukherroub, and W.J. Leigh. J. Photochem. Photobiol. A. In press.
21. Y. Apeloig and M. Karni. J. Am. Chem. Soc. **106**, 6676 (1984).
22. M. Elsheikh, N.R. Pearson, and L.H. Sommer. J. Am. Chem. Soc. **101**, 2491 (1979).
23. P. Jutzi and P. Langer. J. Organomet. Chem. **202**, 401 (1980).
24. W.J. Leigh, C.J. Bradaric, and G.W. Sluggett. J. Am. Chem. Soc. **115**, 5332 (1993).
25. N. Auner and J. Grobe. J. Organomet. Chem. **188**, 25 (1980).
26. R.C. Weast (*Editor*). CRC handbook of chemistry and physics. 75th ed. CRC Press, Boca Raton, Fla. 1995. pp. 6–241.
27. A. Sekiguchi and W. Ando. Organometallics, **6**, 1857 (1987).
28. N. Auner and J. Grobe. J. Organomet. Chem. **197**, 147 (1980).
29. N. Wiberg, G. Wagner, G. Muller, and J. Riede. J. Organomet. Chem. **271**, 381 (1984).
30. C. Kerst, M. Byloos, and W.J. Leigh. Can. J. Chem. **75**, 975 (1997).
31. V.D. Kiselev and J.G. Miller. J. Am. Chem. Soc. **97**, 4036 (1975).
32. A.A. Gorman, G. Lovering, and M.A.J. Rodgers. J. Am. Chem. Soc. **101**, 3050 (1979).
33. N.J. Turro, G.F. Lehr, J.A. Butcher, R.A. Moss, and W. Guo. J. Am. Chem. Soc. **104**, 1754 (1982).
34. I.R. Gould, N.J. Turro, J. Butcher, Jr., C. Doubleday, Jr., N.P. Hacker, G.F. Lehr, R.A. Moss, D.P. Cox, W. Guo, R.C. Munjal, L.A. Perez, and M. Fedorynski. Tetrahedron. **41**, 1587 (1985).
35. K.N. Houk, N.G. Rondan, and J. Mareda. Tetrahedron, **41**, 1555 (1985).
36. R.A. Moss, W. Lawrynowicz, N.J. Turro, I.R. Gould, and Y. Cha. J. Am. Chem. Soc. **108**, 7028 (1986).
37. R.A. Moss. Acc. Chem. Res. **22**, 15 (1989).
38. J.E. Baggott, M.A. Blitz, H.M. Frey, and R. Walsh. J. Am. Chem. Soc. **112**, 8337 (1990).
39. M.A. Blitz, H.M. Frey, F.D. Tabbutt, and R. Walsh. J. Phys. Chem. **94**, 3294 (1990).
40. Y. Chen, A. Rauk, and E. Tschuikow-Roux. J. Phys. Chem. **95**, 9900 (1991).
41. J.E. Jackson, N. Soundararajan, M.S. Platz, M.P. Doyle, and M.T.H. Liu. Tetrahedron Lett. **30**, 1335 (1989).
42. H. Mayr, R. Schneider, and U. Grabis. J. Am. Chem. Soc. **112**, 4460 (1990).
43. M. Patz, H. Mayr, J. Bartl, and S. Steenken. Angew. Chem. Int. Ed. Engl. **34**, 490 (1995).
44. K.M. Baines and W.G. Stibbs. Adv. Organomet. Chem. **39**, 275 (1996).
45. J.W.F.L. Seetz, B.J.J. Van De Heisteeg, G. Schat, O.S. Akkerman, and F. Bickelhaupt. J. Org. Chem. **277**, 319 (1984).
46. K. Izutsu. Acid–base dissociation constants in dipolar aprotic solvents. IUPAC Chemical Data Series no. 35. Blackwell Scientific Publications, Oxford. 1990. p. 17.
47. W.J. Leigh, M.S. Workentin, and D. Andrew. J. Photochem. Photobiol. A: **57**, 97 (1991).